4 Photodissociation in the gas phase

Hiroyasu Sato*

University of the Air, Mi'e Study Center, 1234 Kozu-beta, Isshinden Tsu 514-0061, Japan. E-mail: satlaser@ztv.ne.jp; Fax: 81 59 225 8078; Tel: 81 59 225 8078

Photodissociation dynamics investigations published in 2003 have been reviewed. Some of the highlights are the measurement of dissociation rate of benzene, the manifestation of ring isomerization prior to photodissociation, the discovery of conformation-specific dissociation dynamics, and the studies on halogen-containing compounds in relation to the ozone-deficit problem, to name a few.

1 Scope

This review addresses recent advances in the title field in 2003. Among other methods, imaging techniques including multimass imaging, Rydberg (H) atom photofragment translational spectroscopy, femtosecond pump–probe photoelectron spectroscopy, and time-resolved Fourier-transform IR emission spectroscopy, have been widely applied.

Quite naturally, the progress made in 2003 stands on the basis of a wealth of achievements which have been done before. A very brief introduction on the motives of research and the methodology used is presented in the following two sections. Space limitation does not allow detailed interpretation. Readers are referred to the preceding review by the author[1] and to outstanding books.[2–4]

2 Motives of research and information sought

Photodissociation dynamics concerns the mechanisms of photodissociation reactions investigated in atomistic detail, tracing the time evolution of every microscopic step, as far as possible. The main motive of such research is to clarify the true nature of the chemical reactions. The photodissociation reaction "photoexcited molecules → photofragments" corresponds to the latter half of the bimolecular chemical reaction "reactant(s) → transition state → product(s)", where the photoexcited molecules correspond to the transition state.

The information is usually sought for the entity of product(s) and intermediate(s), partition of the excess energy ("available energy") $E_{\mathrm{avl}} = h\nu - D$, where D is the bond dissociation energy, among many degrees of freedom, translational and internal

DOI: 10.1039/b313672h

(electronic, vibrational and rotational), of the fragments, and their angular distributions. The fractions of available energy among these degrees of freedom, denoted f_T, f_{INT} (f_{el}, f_V, f_R), respectively (total = 1), are denoted energy disposal. When the vibrational or rotational state distribution can be described by Boltzmann distributions, vibrational (T_v) or rotational temperature (T_R) is used to describe the distribution.

Vector correlations among many directional properties, such as transition moments ($\boldsymbol{\mu}$), recoil velocity ($\boldsymbol{V}$) and rotational angular momentum ($\boldsymbol{J}$) of the fragments, are also studied. The anisotropy parameter (β) refers to the angular distributions of recoiling fragments in relation to the polarization vector of the dissociating laser light.

3 Methodology

A brief list of typical methods in our arsenal is given below. This is partly for the description of the abbreviated terms. Lasers (mainly pulsed), are used both to initiate the reactions and to probe the reaction products. Ultraviolet (UV) lasers, such as excimer lasers, the third or fourth harmonics of solid lasers (*e.g.* Nd:YAG or titania-sapphire), and the second harmonics of dye lasers, are necessary to break chemical bonds in the one-photon process, since the dissociation energy (D) of typical bonds lies in the UV region. Femtosecond (fs) lasers are very helpful in following the course of reactions in the real time.

Synchrotron radiation (SR) is used in the vacuum ultraviolet (VUV) region. Infrared (IR) lasers are used in some cases. They are mostly of difference-frequency generation or optical parametric oscillator (OPO) type. Free electron lasers (FELs) are a convenient source of tunable IR light.

Laser-induced fluorescence (LIF), photoionization (PI), and resonance-enhanced multiphoton ionization (REMPI) are used to probe nascent vibrational–rotational state distributions of photofragment(s). In photofragment translational spectroscopy (PTS), time of flight (TOF) of photofragments is used to determine their translational energy distributions and provide information on energy disposal. When photoproducts are formed in spin multiplet states such as iodine atoms in the ground state (I, $j = 3/2$) and spin-excited state (I*, $j = 1/2$), or in the lambda doublet states, their distributions provide further aspects of product distribution.

The ion imaging technique is a combination of a molecular beam, MPI, and detection of ions on a two-dimensional detector. MPI detection of hydrogen atom (H) fragments using the high Rydberg excited levels of H atoms as the resonance intermediate states, denoted H (Rydberg) atom photofragment translational spectroscopy, has been conveniently used due to its high resolution. Vibrationally mediated photodissociation (VMP) is a double-resonance technique, in which the molecules are first excited to some of the vibration–rotational excited states corresponding to their fundamental bands or overtones/combination bands, and subsequently photodissociated by a second (UV) laser photon.

Photofragment yield (PFY) spectra are action spectra for particular photoproduct(s), and photofragment emission yield spectra (PHOFREY) are for a particular excited state of the photoproducts.

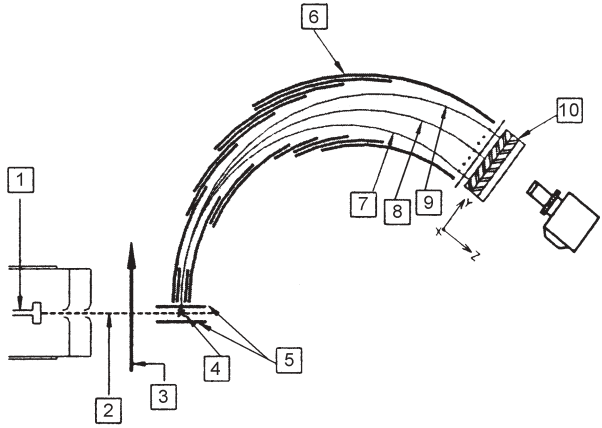

Fig. 1 Schematic drawing of the multimass ion imaging detection system: (1) nozzle; (2) molecular beam; (3) photolysis laser beam; (4) VUV laser beam (perpendicular to the plane of the paper); (5) ion extraction plates, (6) energy analyzer; (7), (8), (9) simulation ion trajectories; (10) two-dimensional detector (see text). (Reprinted with permission from *J. Chem. Phys.*, 2003, **119**, 7701.[5])

Only one of the new techniques (multimass spectroscopy developed by Ni and Y. T. Lee) is explained below, according to the paper by Tsai *et al.*[5] (see Fig. 1). The apparatus consists of a molecular beam, a photolysis laser beam, a VUV probe laser beam, a mass spectrometer, and a two-dimensional ion detector. The molecular beam, photolysis laser beam, and VUV laser beam are perpendicular each other. The crossing point of the photolysis laser beam with the molecular beam and that of the VUV laser beam with the molecular beam are not the same; the former is several centimeters upstream relative to the latter.

Molecules in the molecular beam are photodissociated by a photolysis laser beam. The dissociation products expand into a large sphere on their flight to the ionization region, and then ionized by a VUV laser pulse. The distance and time delay between the photolysis laser pulse and the VUV laser pulse are set such that the time delay matches the arrival of the undissociated molecules. This time delay ensures that the VUV laser beam passes through the center of the fragment sphere, and the velocity distribution of the fragments is measured in the center of mass frame.

A pulsed electric field extracts the ions into a mass spectrometer. The entrance of the mass spectrometer has a long slit parallel to the VUV laser beam.

The mass spectrometer is basically a radial cylindrical energy analyzer. Since the VUV laser beam passes through the center of the fragment sphere, fragments ionized by the VUV laser have recoil velocity along in the direction of the VUV laser beam axis. At the exit port of the energy analyzer, a two-dimensional ion detector is used to detect ion position and intensity distributions. In the detector, one direction is the recoil velocity axis (X axis in Fig. 1) and the other is the mass axis (Y axis in Fig. 1).

4 Saturated hydrocarbons

A remarkable progress has been made in the photodissociation studies of small saturated hydrocarbon molecules, by the use of synchrotron radiation (SR) as a light source, along with highly sensitive detection methods of light fragments, such as H and D atoms.

Alkanes

Wu *et al.*[6] photodissociated propane (C_3H_8) at 157 nm. Photofragment translational spectroscopy (PTS) indicated contributions of three channels, atomic hydrogen (H) elimination, molecular hydrogen (H_2) elimination, and methyl radical (CH_3) elimination, with branching ratios of 1, 2.1 and 1.5. The site effects on the H and H_2 elimination was quantified, using four isotopomers $CH_3CD_2CH_3$, $CD_3CH_2CD_3$, $CH_2DCH_2CH_2D$ and $CD_3CD_2CD_3$. The yield of the H elimination from the two terminal CH_3 groups was larger than that from the internal CH_2 group. As for the H_2 elimination sites, internal (2,2-) was dominant, vicinal (1,2-) was less significant, and terminal (1,1- and 1,3-) was minor.

Cycloalkanes

Photodissociation dynamics of cycloalkanes at 157 nm was investigated by Y. T. Lee and Yang's group.[7] Time of flight (TOF) spectra of photofragments from cycloalkanes at $m/z = 1$ (H) and 2 (H_2) were measured. The H_2 elimination from cyclopropane and cyclopentane showed kinetic energy distributions quite different from those of *n*-alkanes. The relative branching ratios for the H and H_2 elimination channels were also determined. The H elimination process was clearly more important for the photodissociation of smaller cyclic alkanes. Dynamics of the photodissociation of cycloalkanes was strongly related to the flexibility and the ring strain of cycloalkanes. For *cyclo*-C_3H_6 at 157 nm, these authors used a new apparatus based on the VUV ionization by SR. Observed channels were C_3H_5 + H, C_3H_4 + H_2/2H, C_2H_4 + CH_2, and C_2H_3 + CH_3, with a branching ratio 0.14, 0.01, 0.68 and 0.17. Among these products, H atom products were possibly produced *via* a synchronous, concerted 2H elimination process, while other channels were all binary dissociation process.

5 Unsaturated hydrocarbons (aliphatic)

Ethylene

Ethylene ($H_2C{=}CH_2$) is a prototypical alkene molecule, important in astrophysics, combustion and atmospheric sciences. Intermediacy of the ethylidene intermediate is an interesting issue.

The dissociation of ethylene under the excitation by a high energy photon involves

different dissociation channels:

$$C_2H_4 + h\nu \rightarrow HC{\equiv}CH + H_2 \quad (5.1)$$

$$\rightarrow H_2C{=}C{:} + H_2 \quad (5.2)$$

$$\rightarrow H_2C{=}CH + H \quad (5.3)$$

$$\rightarrow HC{\equiv}CH + H + H \quad (5.4)$$

The relative branching ratio for the atomic and molecular hydrogen elimination channel is an interesting issue. For the atomic hydrogen elimination, the triple dissociation channel is complicated.

Lin *et al.*[8] investigated both the atomic and molecular hydrogen elimination at 157 nm, using five different isotopomers, *i.e.*, C_2H_4, C_2D_4, CD_2CH_2, *cis*- and *trans*-CHDCHD. The 1,1-, 1,2-*cis* and 1,2-*trans* D_2 elimination processes showed significant differences in the kinetic energy distributions, indicating that the dynamics of D_2 elimination from different sites were quite different. The difference may partly arise from the different transition states. That of 1,2-elimination was theoretically believed to be the ethylidene radical ($:CHCH_3$).

The photodissociation of ethylene in the higher energy region was explored by O'Reilly *et al.*,[9] using 106–58 nm (11.7–21.4 eV) SR. Emission from the excited fragments CH* ($A\,^2\Delta$), and CH* ($B\,^2\Sigma^-$) were measured. Their formation thresholds were identified and associated with two dissociation channels CH* + CH_3 and CH* + CH + H_2. The intermediacy of ethylidene was proposed.

Photodissociation dynamics of propene was studied by Lee *et al.*[10] at 157.6 nm. The observed eleven photofragments were ascribed to eight (five binary and three triple) dissociation channels: C_3H_5 + H, C_3H_4 + H + H, C_3H_4 + H_2, C_3H_3 + H_2 + H, C_2H_4 + CH_2, C_2H_3 + CH_3, C_2H_2 + CH_4, and C_2H_2 + CH_3 + H. The complicated multichannel dissociation process showed a propensity towards triple dissociations, notably the C_2H_2 + CH_3 + H channel.

Acetylene

Kono *et al.*[11] photolyzed acetylene in the 135.3–130.8 nm range, corresponding to the excitation to ($\tilde{D}\,^1\Pi_u$, $\tilde{E}\,^1A$, $\tilde{F}\,^1\Sigma_u^+$) states. Photofragment emission yield spectroscopy of C_2H ($\tilde{A}\,^2\Pi$, $\tilde{B}\,^2A'$) revealed that the $\tilde{D}\,3_1^1$, $\tilde{D}\,1_1^1 3_1^1$, $\tilde{F}\,3_1^1$, and $\tilde{F}\,1_1^1 3_1^1$ bands were broadened significantly compared with the corresponding origin bands, indicating that the dissociation was accelerated significantly by the antisymmetric C–H stretch (ν_3) in the $\tilde{D}$ and $\tilde{F}$ states. Yamakita *et al.*[12] studied predissociation of acetylene excited in the $\tilde{A}\,^1A_u$ state around the adiabatic dissociation threshold (47 000–50 600 cm^{-1}) by LIF and H-atom action spectra. The line intensities of the H-atom action spectra increased at the higher excitation energies, indicating the more efficient predissociation. The lifetime was shortened from 100 ps at 47 000 cm^{-1} to 25 ps at 50 600 cm^{-1}, which exceeds the adiabatic dissociation threshold of the $\tilde{A}$ state by 933 cm^{-1}.

Zamith *et al.*[13] investigated the predissociation of highly excited states in acetylene by time-resolved photoelectron spectroscopy. Electronic states lying in the 4s–3d Rydberg region were excited with one femtosecond laser pulse. They were able to

extract short decay lifetimes through time-resolved photoelectron spectroscopy. The lifetimes measured were 20–200 fs for HCCH, and those in DCCD were somewhat longer (about 600 fs).

Acetylene derivatives

Allene ($H_2C{=}C{=}CH_2$) and propyne ($H_3C{-}C{\equiv}CH$) are isomers of each other and identified in the atmospheres of the outer planets and in interstellar clouds. Near-UV photodissociation at 203.3, 209.0 and 213.3 nm was studied by Qadiri *et al.*,[14] using the H (Rydberg) atom photofragment translational spectroscopy. Contrary to the previous studies at slightly higher energy (193 nm), the translational energy spectra associated with the H atom product forming channel in both molecules were essentially identical. Such an behavior could be interpreted in terms of internal conversion to, and isomerization on, the ground state potential energy surface to H_2CCCH (propargyl) + H.

Photodissociation of propyne ($HC{\equiv}CCH_3$, $HC{\equiv}CCD_3$, $DC{\equiv}CCH_3$) at 157 nm was investigated by Harich *et al.*[15] The corresponding dynamics was inherently complex. Hydrogen atom elimination occurred from both the CH_3 group and the CCH (ethynyl) group. The former process (relative contribution 0.27) was a single process, while the latter showed two distinct channels (fast H:slow H = 0.30:0.43). Molecular hydrogen elimination was also observed, but with a much smaller yield compared to the atomic hydrogen elimination. Comparison of the H_2, HD, D_2 products from various deuterated molecules showed that the process was not sensitive to the origin of two hydrogen atoms (*i.e.*, scrambling prior to dissociation was important). Two different C–C bond breaking processes were observed: $HC{\equiv}C + CH_3$ and $CH_2 + C_2H_2$ in the ratio of 2.2:1. The existence of CH_2 further indicated that the isomerization of propyne was significant prior to dissociation.

Quite recently, Qadiri *et al.*[16] studied the 193.3 and 121.6 nm photolysis of $H_3CC{\equiv}CH$, $D_3CC{\equiv}CH$ and $H_2C{=}C{=}CH_2$ (allene) by H (D) Rydberg atom PTS. For the 193.3 nm-photolysis, the total kinetic energy release (TKER) spectra of photofragments resulting from these molecules were found to be essentially identical. The observed energy disposal and the isomer independence were rationalized by the assumption that the fragmentation of both molecules are preceded by internal conversion (IC) to, and the isomerization on, the ground (S_0) state. At 121.6 nm, however, the TOF and TKER of H from propyne were significantly different from those from allene. Two competing pathways were assumed for propyne, one from the prepared excited states or ''propyne like'' state, and the other (giving the slower distribution of H (D) atoms) *via* the IC and isomerization.

6 Halogenated hydrocarbons, saturated

Chlorine-containing species

In the stratosphere, Cl-containing haloalkanes are dissociated by UV or VUV irradiation to produce Cl atoms, which can then lead to the catalytic decomposition

of ozone. Methyl chloride is the largest natural source (*e.g.* from tropical plants) of stratospheric chlorine compounds. Lin *et al.*[17] photodissociated CH_3Cl at 157.6 nm. Products were probed by VUV photoionization by SR. In addition to channels (6.1) and (6.2), these authors found evidence for channel (6.3).

$$CH_3Cl + h\nu \rightarrow CH_3 + Cl \quad (6.1)$$

$$\rightarrow H + CH_2Cl \quad (6.2)$$

$$\rightarrow CH_2(\tilde{X}\,^3B_1/\tilde{a}^1A_1) + HCl \quad (6.3)$$

CH_3CFCl_2 has been used as a replacement for $CFCl_3$ and for $CFCl_2CF_2Cl$. Although its production was stopped in 1996, the release into atmosphere still continues because of the long-term use of the previously manufactured products. Läuter *et al.*[18] determined the absolute quantum yield of chlorine and hydrogen atoms at 193 nm. The total chlorine atom quantum yield (Φ_{Cl+Cl^*}) was found to be 1.01, and the H atom quantum yield $\Phi_H = 0.04$.

Bromine-containing species

Atomic bromine exhibits a 40 times more powerful ozone depletion potential than a chlorine atom. Jackson's group published several papers in this field. Huang *et al.*[19] photolyzed $CH_2Br_2^+$ at 355 nm. The translational energy distribution showed that CH_2Br^+ fragment was formed in highly vibrational states. Xu *et al.*[20] studied photodissociation of bromoform ($CHBr_3$) at 267 and 234 nm.

$$CHBr_3 + h\nu \rightarrow CHBr_2 + Br \quad (6.4)$$

$$\rightarrow CHBr + Br_2 \quad (6.5)$$

Besides the atomic dissociation channel (6.4), they found the contribution of the molecular dissociation channel (6.5). The branching ratio of channels (6.4) and (6.5) was 0.74 and 0.26 at 234 nm, respectively. Huang *et al.*[21] photolyzed $CHBr_3^+$ at 308, 355 and 610 nm. The only fragment found in the TOF spectra was $CHBr_2^+$ at 355 and 610 nm. At 308 nm CBr^+ and $CHBr^+$ ions were also found.

Zou *et al.*[22] found Φ_{Br^*+Br} close to 2 on the 193 nm photodissociation of 1,2-dibromotetrafluoroethane ($BrCF_2CF_2Br$). Following the rupture of one C–Br bond, the second C–Br bond was significantly weaker than a typical C–Br bond, due to the energy associated with forming the C=C bond that largely offsets the energy necessary to break the second C–Br bond. Photodissociation of CH_2Br_2 (DBM), 1,1- and 1,2-$C_2H_4Br_2$ (DBE) was studied at 248 nm by Lee *et al.*,[23] using product translational spectroscopy. 1,2-DBE dissociated into products Br (fast), Br (slow) and C_2H_4 in a concerted manner, while simple C–Br bond scission was observed for DBM and 1,1-DBE. The behavior of 1,2-DBE was discussed in terms of the weakness of the C–Br bond strength in the β-bromomethyl radical, that a rapid scission of the second C–Br bond occurred asynchronously with the cleavage of the first C–Br bond.

Iodine-containing species. Concerted *vs.* sequential dissociation

The advances in femtosecond chemistry made possible the distinction of concerted *vs.* sequential detachment processes. Farmanara *et al.*[24] analyzed the 267 nm-photodissociation of CF_2I_2 by femtosecond time-resolved photoelectron spectroscopy (pump–probe technique combined with the photoelectron–photoion coincidence detection (PEPICO)). They observed that fast (30 fs) relaxation process precedes dissociation (100 fs). The observed products were CF_2, I_2, I, with no CF_2I. They concluded that the concerted reaction mechanism was dominant, while the sequential decay with the CF_2I intermediate was negligible.

Femtosecond velocity map imaging of CF_2I_2 at 264 nm enabled Roeterdink and Janssen[25] to follow the molecular detachment, *e.g.* a concerted *vs.* a sequential bond-breaking process, on the time scale of the event. The I_2^+ fragment found at short pump–probe decay ($\leqslant$250 fs) was attributed to one-photon excitation at 264 nm followed by subsequent ionization, I_2^+ found at long pump–probe decay ($\geqslant$500 fs) to two-photon excitation at 264 nm to a highly electronically excited state of the parent, followed by concerted asynchronous dissociation producing a highly internally (rotationally) excited I_2* fragment and subsequent ionization of this highly excited I_2 fragment.

Conformation-specific photodissociation

A very interesting conformation-specific photodissociation was reported by Park *et al.*[26] They succeeded in the selective preparation of the *gauche* and *anti*-conformer of 1-iodopropane ions (1-$C_3H_7I^+$) by coherent VUV mass-analyzed threshold ionization (MATI) of the parent molecules. Then they photodissociated the ions by excitation to the C–I repulsive first excited state by a visible laser pulse (480–700 nm). Substantial difference in the kinetic energy release (0.096 and 0.042 eV for *gauche* and *anti* conformers, respectively) observed for the photodissociation at 607 nm was attributed to conformation-specific dissociation pathways, producing 2-propyl ions and protonated cyclopropane ions from *gauche* and *anti*-conformers, respectively. However, excitation to the S_2 and S_3 excited states did not show conformation-specificity.[27]

7 Halogenated hydrocarbons, unsaturated (aliphatic)

Halogenated ethylenes. Three-center *vs.* four-center dissociation

Time-resolved Fourier transform (FT) IR emission spectroscopy was conveniently used in the study of three-center and four-center elimination channels of halogen-substituted ethylenes. Vinyl chloride (H_2C=CHCl) photodissociation at 193 nm was studied using this technique by Lin *et al.*[28] Vibrationally excited HCl ($v \leqslant 7$) was detected, with the bimodal rotational distribution (T_R = 500 and 9500 K for $v \leqslant 4$). The low-J component was found to exhibit an inverted vibrational population. The high-J and low-J components were attributed to HCl (v, J) produced from three-center and four-center elimination channels, respectively.

The HBr product from photodissociation of vinyl bromide (H_2C=CHBr) at 193 nm

was studied by Liu *et al.*[29] using the time-resolved FT IR emission spectroscopy with 0.5 μs resolution.

$$H_2C{=}CHBr \rightarrow H_2C{=}CH + Br \quad (7.1)$$

$$\rightarrow H_2C{=}C{:} + HBr \text{ (three-centered)} \quad (7.2)$$

$$\rightarrow HC{\equiv}CH + HBr \text{ (four-centered)} \quad (7.3)$$

The nascent distribution of the HBr product was extrapolated to be $T_V = 8690$ K and $T_R = 7000$ K. The vibrational distribution gave a support for the three-centered HBr elimination. Therefore, the HBr product was due to the channel (7.2). The nascent internal energy of vinylidene was deduced to be 24 kcal mol^{-1}. Vinylidene was found to isomerize to acetylene. 2-Chloro-1,1-difluoroethene ($F_2C{=}CHCl$) was studied by Wu *et al.*[30] at 193 nm. Vibration–rotationally resolved emission of HCl ($v \leqslant 3$) and HF ($v \leqslant 4$) indicated that HCl was produced *via* three-center (α,α) elimination, but HF *via* four-center (α,β) elimination.

The stability of the allyl radical ($H_2C{=}CHCH_2$) to C–H scission is an interesting issue. Szpunar *et al.*[31] photodissociated allyl-d_2 iodide ($H_2C{=}CDCH_2I$) at 193 nm, and studied the dynamics of the nascent allyl-d_2 radical by photofragment translational spectroscopy. The stability of the highly rotationally excited allyl-d_2 radical ($H_2C{=}CDCH_2$) to C–D scission was confirmed.

8 Aromatic compounds

Direct determination of slow dissociation rate

The absorption of benzene and alkyl-substituted benzenes in the 190–270 nm region corresponds to the excitation of the phenyl ring. It results in an excited state stable with respect to dissociation. Dissociation occurs following the internal conversion to the highly vibrationally excited ground electronic state ("hot molecule"). The dissociation rate of aromatic compounds has been reported extensively, including toluene, *o*-, *m*-, *p*-xylene, trimethyl-, tetramethylbenzene, *etc*. However, that of the simplest and most important one (benzene) was lacking, since the rate was much slower and difficult to measure accurately.

Tsai *et al.*[32] studied the dissociation rate of hot benzene and d_6-benzene, using the multimass ion imaging technique.[33] The benzene–He or –Ar mixture under collision-free condition was irradiated at 193 or 248 nm and fragment ions were detected *via* VUV laser ionization. The measured values were $1 \pm 0.2 \times 10^5$ and $5 \pm 1 \times 10^4$ s^{-1} for C_6H_6 and C_6D_6, respectively. These authors[34] studied photodissociation of benzotrifluoride ($C_6H_5CF_3$) at 193 nm. The photofragments observed were F and CF_3. The dissociation rate was measured to be 6.2×10^4 s^{-1}.

Ring-opening dissociation

Ring-opening dissociation of d_6-benzene was reported by Tsai *et al.*[35] In addition to the major-channel of D-atom elimination from one-photon excitation, elimination of

two D atoms and two ring-opening dissociation channels, $C_6D_6 \rightarrow CD_3 + C_5D_3$ and $C_6D_6 \rightarrow C_2D_3 + C_4D_3$, resulting from two-photon dissociation, was observed. Fluorobenzene was found to give HF and DF fragments *via* a four-center reaction mechanism (Huang *et al.*[36]).

Dissociation through the exited state

Dissociation of benzene occurs following the internal conversion to the highly vibrationally excited ground electronic state ("hot molecule"), as mentioned above. However, photofragment translational energy distributions of ethylbenzene obtained by Huang *et al.*[37,38] at 248 nm (S_1), using multimass ion imaging techniques, were composed of two components, indicating that some 75% of molecules dissociate through the electronic excited state, and 25% through a hot molecule mechanism.

Benzene derivatives

o- *m*- and *p*-Chlorotoluene were photodissociated at 193 nm by Lin *et al.*[5] In addition to Cl atom elimination (the major channel), photofragments corresponding to the reactions of $C_6H_4ClCH_2 + H$ and $C_6H_4Cl + CH_3$ were observed. *o*- *m*- and *p*-Dibromobenzene and 1,3,5-tribromobenzene were photodissociated at 266 nm by Kadi and Davidsson[39] using femtosecond pump–probe spectroscopy.

Photoisomerization

Photoisomerization of toluene in a molecular beam (collision-free) was observed in the 193-nm photolysis experiments of Lin *et al.*,[40] using isotope-labeled toluene ($C_6H_5CD_3$ and $C_6H_5{}^{13}CH_3$). For $C_6H_5CD_3$, CD_2H, CDH_2, CH_3 and their heavy fragment partners were observed, in addition to the major channels ($C_6H_5CD_3 \rightarrow C_6H_5CD_2 + D$, $C_6H_5 + CD_3$). For $C_6H_5{}^{13}CH_3$, $^{13}CH_3$ and CH_3 and their heavy fragment partners were observed. These results showed that 25% of the excited toluene isomerizes to a seven-membered ring (cycloheptatriene) and then rearomatizes prior to dissociation.

Azulene ($C_{10}H_8$) was photolyzed at 193 nm by Lin *et al.*,[41] using the multimass ion imaging technique. The result showed that most of the azulene molecules isomerize to naphthalene in the ground electronic state prior to dissociation.

Lee *et al.*[42] photodissociated styrene ($C_6H_5CH{=}CH_2$) at 193 nm. The result showed predominance of molecular elimination of C_2H_2 and H_2. In the latter case, an intermediate bicyclo[4.2.0]octa-2.4,7-triene is formed.

$$C_6H_5CH{=}CH_2 + h\nu \rightarrow C_6H_6 + C_2H_2 \quad (8.1)$$

$$\rightarrow C_8H_6 + H_2 \quad (8.2)$$

Nitrobenzene was photolyzed in the gas phase at 266 nm by Li *et al.*[43] monitoring the NO ($X\,^2\Pi$) product using LIF. *Ab initio* calculations were made to characterize the

transition state and to determine the barrier height for the rearrangement of nitrobenzene to phenyl nitrite (C_6H_5ONO). UV photodissociation of nitrosobenzene was studied by Seiler and Dick[44] by detecting the NO fragments by LIF.

Laser-aligned molecule

Photodissociation of laser-aligned iodobenzene was reported by Poulsen *et al.*[45] The yield of I photoproducts, detected by REMPI, was enhanced up to a factor of 2.7 when the dissociation laser was polarized parallel instead of perpendicular to the alignment laser polarization.

9 Cyano compounds

Lyman-α (123.6 nm) photodissociation of HCN and DCN was reinvestigated by Cook *et al.*,[46] using H (D) Rydberg atom TOF spectroscopy. Although the previous assignment of substantial branching to H + CN ($A\,^2\Pi$, $v = 0$) was confirmed, additional structure attributable to CN ($A\,^2\Pi$, $v = 4$–9, $N = 26$–41) and CN ($B\,^2\Sigma^+$), $v = 0,1$ was found. These led to an improved value for the dissociation energy D_0(H–CN) = 43710 ± 70 cm^{-1}. Interestingly, the anisotropy parameter β was found to become increasingly parallel with increasing CN internal energy.

Photodissociation of cyclopropyl cyanide (*cyclo*-C_3H_5CN) at 193 nm was studied by Park and coworkers[47] by LIF of the CN ($X\,^2\Sigma^+$, $v = 0, 1$) fragments. From energetics for various product channels, it was concluded that cyclopropyl cyanide dissociates into an allyl and CN radicals resulting from ring opening prior to dissociation.

The CN product channel from the photodissociation (at 193 nm) of methacrylonitrile ($H_2C{=}C(CH_3)CN$) and 2-butenenitrile was also studied by these authors.[48] The CN ($X\,^2\Sigma^+$) internal (rotational) and translational energy distributions of both molecules were well represented by statistical prior calculations, assuming CN and allyl (rather than the propenyl isomer) products. It was concluded that methacrylonitrile dissociates in the ground electronic state *via* allyl cyanide formed by CN and H atom migration prior to dissociation.

In the 193 nm photodissociation of carbonyl cyanide $CO(CN)_2$, Huber and coworkers[49] observed two energetically different CN radicals, a rotationally and vibrationally hot one ($T_R \approx 2300$ K, $T_V \approx 3600$ K) and a cold one exclusively in $v = 0$ with $T_R \approx 410$ K. The hot one, together with OCCN, was assigned to α-cleavage, while the cold one was from the spontaneous secondary decay OCCN → CO + CN. The three-body decay was sequential. No evidence for a concerted three-body process was obtained.

The photodissociation dynamics of NCNO at 520 and 532 nm was studied by McGivern and North,[50] using transient frequency modulation Doppler spectroscopy of the CN fragment. They observed that the ***v*–*J*** correlation was small (near zero), indicative of an approximate *K*-scrambling (see below, section 16). Gas-phase Raman spectra of NCNCS and its photolysis product, isocyanogen (CNCN), were reported by Li *et al.*[51]

10 Carbonyl compounds

Ketene

Ketene (CH_2CO) photodissociation at 193.3, 203.3, 209 and 213.3 nm was studied by Feltham *et al.*[52] The speed and angular distributions of H atom products were probed using H Rydberg atom PTS. Absorption to the $^1B_1$ excited state was followed by internal conversion to high-lying vibrational levels of ground state, and subsequent unimolecular decay led to the observed H (+ HCCO) products. The kinetic energy distributions were qualitatively reproduced by the statistical adiabatic product distribution (SAPD) method of Cole and Balint-Kurti.

Glyoxal

Chen and Zhu[53] used cavity ring-down spectroscopy to investigate the gas-phase photolysis of glyoxal in the wavelength range 290–420 nm. The dependence of the photoproduct (HCO) quantum yield on the photodissociation wavelength, glyoxal pressure, and nitrogen buffer gas pressure was measured. The peak quantum yield was 2.01 $\pm$ 0.08. Chen *et al.*[54] determined the threshold for formation of HCO from *trans*-glyoxal based on the measurement of fluorescence excitation spectra. The threshold was determined to be 394.4 nm.

Acetone

The long-standing issue concerning the concerted *vs*. sequential breakage of two α-C–C bonds was settled in favor of the stepwise mechanism using femtosecond time-resolved experiments. Zewail's group published a series of four papers[55–58] on femtosecond pump-and-probe TOF spectrometry on Norrish Type-I reactions of acetone and related ketones. The α-cleavage dynamics of acetone following the excitation to the S_1 (n, π^*) state[55] was observed to occur on the nanosecond time scale. The energy barrier along the α–CC bond dissociation was calculated to be 18 kcal mol^{-1}. The dynamics below the barrier was interpreted to be governed by a rate-limiting S_1–T_1 intersystem crossing process, followed by α-cleavage on the T_1-surface.

In the second paper of this series, Diau *et al.*[56] studied anomalous predissociation dynamics of cyclobutanone (*cyclo*-C_3H_6CO) by the femtosecond pump–probe method. Three isotopomers were used: [D_0], 3,3-[D_2], 2,2,4,4-[D_4]cyclobutanone. The decay times of fragment transients, 5.0 $\pm$ 1.0, 9.0 $\pm$ 1.5, and 6.8 $\pm$ 1.0 ps, respectively, were shorter than observed for other aliphatic ketones by three orders of magnitude at the same, or even much higher, excitation energies. They reflect the extremely low (*ca*. 2 kcal mol^{-1}) energy barrier of cyclobutanones along the α-CC bond breakage (ring-opening) reaction coordinate. The prominent isotope effect was attributed to the importance of ring-puckering motion. Femtochemistry of highly excited ketones was studied in the third[57] and fourth[58] paper from Zewail's group. The dissociation reaction of acetone on the S_2 (n, 3s) Rydberg state, generally

assumed to follow a similar pathway to the S_1 excitation, *i.e.*, on the ground electronic state, was reinterpreted along the "new" mechanism that the dissociation occurs on the S_1 surface.

Chen *et al.*[59] studied the S_2 (n, 3s) Rydberg state at 195 nm, and gave a supporting evidence for Zewail's "new" mechanism (Fig. 2). Tang *et al.*[60] reported the photodissociation reaction of acetone in an intense femtosecond laser field (10^{13}–10^{14} W cm^{-2}). The stepwise, field-assisted dissociation mechanism was verified by analyzing the TOF patterns at different laser intensities.

Ketones and carbonic acids

Photodissociation dynamics of dicyclopropyl ketone was studied at 193 nm by Clegg *et al.*,[61] using time-resolved FTIR spectroscopy and photofragment ion imaging. The photoproducts were C_3H_5 + CO + C_3H_5. The C_3H_5 product was not cyclopropyl radicals. It was found that the excited dicyclopropylketone undergoes ring-opening isomerizations to form diallyl ketone, followed by dissociation producing allyl radicals and carbon monoxide.

Ultrafast dynamics of the 3s Rydberg state of three ketones CH_3CO–R, R = C_2H_5, C_3H_7 and *iso*-C_4H_9, was studied by Zhong *et al.*,[62] using ultrafast photoionization spectroscopy. The 3s state lifetimes were similar (2.5–2.9 ps). Those of the acetyl

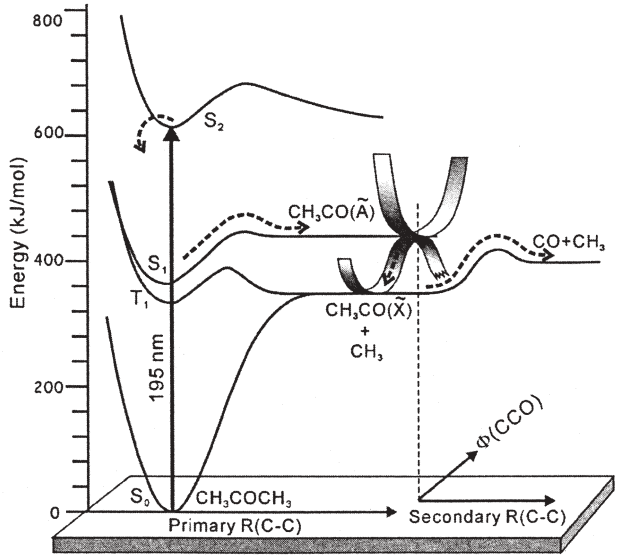

Fig. 2 Schematic potential energy profiles of acetone along the primary and secondary α-C–C dissociation coordinates. The axis perpendicular to R(C–C) represents the CCO bending coordinate. The dashed curved arrows represents the reaction pathway for the "new" mechanism (see text; reprinted with permission from *Chem. Phys. Lett.*, 2003, **380**, 411[59]).

radical were 8.6, 15 and 23 ps for R = C_2H_5, C_3H_7 and *iso*-C_4H_9, respectively, suggesting that for larger R more vibrational freedom compete for the excess energy so that less energy is partitioned into the internal energy of the acetyl radical. Photodissociation dynamics at 266, 248, and 193 nm of acetylacetone, which exists predominantly as an enolic form [$H_3CCOCH{=}C(OH)CH_3$] in the gas phase, was explored by Upadhyaya *et al.*[63] Dhanya *et al.*[64] studied OH formation from pyruvic acid ($CH_3COCOOH$) at 193 nm.

11 Free radicals

Halogenated methyl radicals

Halogenated methyl radicals are important in stratospheric chemistry, since they provide an additional source of photolytic halogen atoms. Reisler's group[65,66] photolyzed chloromethyl radicals (CH_2Cl) in the wavelength range 312–214 nm. Among the dissociation channels,

$$CH_2Cl \rightarrow Cl + CH_2 \quad (11.1)$$

$$\rightarrow H + CHCl \quad (11.2)$$

channel (11.1) was identified as a major one. With 312–247 nm photolysis, the angular distributions were typical of a perpendicular transition ($\beta = -0.7$), and the main products was $CH_2(\tilde{X}\,^3B_1)$ + $Cl(^2P_{3/2})$. The available energy was partitioned preferentially into translational degrees of freedom. Hot band transitions were prominent even in the molecular beam, indicating that the geometries of the ground and excited states of CH_2Cl must be very different. With 240–214 nm photolysis, $\beta = 1.2$ (parallel transition), and the predominant products were $CH_2(\tilde{a}\,^1A_1)$ + $Cl(^2P_{3/2,1/2})$. A large fraction of the available energy was partitioned into internal energy of $CH_2(\tilde{a}\,^1A_1)$. In the region in between (243–235 nm), the Cl images indicated the participation of two transitions, perpendicular ($1\,^2A_1$–$1\,^2B_1$) and parallel ($2\,^2B_1$–$1\,^2B_1$). H-atoms from channel (11.2) was identified as a minor product. Its angular distribution exhibited perpendicular character only.

The hydroxymethyl radical

Photodissociative spectroscopy of the hydroxymethyl radical (CH_2OH) in its two lowest excited electronic states, 3s and $3p_x$, was reported by Feng *et al.*,[67,68] using depletion, REMPI and photofragment yield (PFY) methods. The result on CH_2OD showed that only the O–D bond scission pathway was important near the onset of the 3s state, while both H and D products were detected following excitation to the $3p_x$ state. On the former excitation (352.5 nm), the fraction of available energy into the translational degree of freedom (f_T) was 0.69, and the recoil anisotropy was negative ($\beta_{eff} = -0.7$), consistent with the perpendicular nature of the transition.

The NCO radical

NCO is an intermediate in the combustion of nitrogeneous fuels in air. It has also been proposed as a key intermediate in the RAPRENOs (rapid reduction of NO_x) process. The NCO radical was studied by two groups. The geometry of the excited state was inferred from high f_R values. Hoops *et al.*[69] used fast beam PTS. Excitation of the 1_0^2, 3_0^1, $1_0^2 3_0^2$ transitions of the $\tilde{B}\,^2\Pi$–$\tilde{X}\,^2\Pi$ band produced exclusively N(^{4}S) + CO, while excitation of the $1_0^3 3_0^3$ transition yielded primarily N(^{2}D) + CO photoproducts. The N(^{2}D) + CO distribution could be fit by phase space theory, while the higher degree of CO rotational excitation for N(^{4}S) + CO products implied that NCO passes through a bent geometry upon dissociation. Gomez *et al.*[70] photolyzed NCO at 193 nm, and detected N(^{2}D, ^{2}P) and CO($^1\Sigma^+$) products by VUV LIF. The CO vibrational distribution was modeled with prior distributions for each of the channels with coproducts N(^{4}S, ^{2}D and ^{2}P). For the N(^{2}D) + CO($^1\Sigma^+$) channel, the average energy disposal ($f_T = 0.08$, $f_V = 0.24$, $f_R = 0.68$) suggested that the geometry of the dissociation state of NCO is likely bent.

12 Nitrogen dioxide and halogen nitrates

Nitrogen dioxide

The photochemistry of NO_2 plays a critical role in the chemistry of the troposphere and stratosphere. The relevant reaction channels are

$$NO_2 + h\nu \rightarrow O(^3P) + NO(X\,^2\Pi),\ \lambda_{th} = 398\ \text{nm} \quad (12.1)$$

$$\rightarrow O(^1D) + NO(X\,^2\Pi)\ 244\ \text{nm} \quad (12.2)$$

$$\rightarrow N(^4S) + O_2(^3\Sigma^-)\ 275\ \text{nm} \quad (12.3)$$

Richter *et al.*[71] photodissociated NO_2 at 212.8 nm. The products were predominantly O(^{1}D) + NO($X\,^2\Pi$, $v = 3$). In the 193-nm photodissociation, Sun *et al.*[72] obtained $O(^1D)/\{O(^1D) + O(^3P)\} = 0.55 \pm 0.03$, and the rate constant $k[O(^1D) + NO_2] = (1.5 \pm 0.3) \times 10^{-10}\ cm^{-3}\ s^{-1}$. Im and Bernstein[73] studied in the range 217–237 nm. At 226 nm, NO($X\,^2\Pi$) products were in the vibrational ground state, and rotationally cold ($T_R = ca.$ 30 K). Most of the excess energy should be released to the translational degrees of freedom of the products.

Stolyarov *et al.*[74] measured the rate constant $k(E)$ immediately above the dissociation threshold (25 128.57 $\pm$ 0.05 cm^{-1} or 397.95 nm) by recording the LIF of NO. They found a rapid increase of $k(E)$ from $\sim 2 \times 10^{10}$ to $\geqslant 1.3 \times 10^{11}\ s^{-1}$ within 25 cm^{-1} of the reaction threshold, and reported that it could not be understood on the basis of current theory. However, Abel *et al.*[75] commented that the data of Stolyarov *et al.* can be explained by quantum mechanical calculations on the global three-dimensional potential energy surface.

Morrell *et al.*[76] studied the 248 nm photolysis of NO_2/N_2O_4 using time-resolved FTIR emission. The photolysis of NO_2 produced the $\Delta v = -1, -2$ fundamental and

overtone bands of NO ($X\,^2\Pi$), and a broad Gaussian-type distribution in the vibrational levels $v = 2$–8.

Halogen nitrates

Chlorine nitrate ($ClONO_2$) is one of the most important temporary reservoir of reactive chlorine. Zou *et al.*[77] studied photodissociation of $ClONO_2$ at 235 nm. Several channels are accessible:

$$ClONO_2 + h\nu \rightarrow ClO + NO_2 \quad (12.4)$$

$$\rightarrow Cl + NO_3 \quad (12.5)$$

$$\rightarrow ClONO + O \quad (12.6)$$

Although the ClO–NO_2 bond is the weakest in the $ClONO_2$, previous experimental studies reported that the channel (12.4) is of minor importance. Zou *et al.* have now determined the total Cl atom quantum yield to be 0.42 and a ClO quantum yield of 0.58, on the basis of simulations to their TOF data. Photodissociation of bromine nitrate ($BrONO_2$) was studied by Soller *et al.*[78]

13 Photodissociation of vibrationally excited molecules (IR-mediated photodissociation)

In the vibrationally mediated photodissociation (VMP) studies, molecules are first excited to vibrational fundamental or overtone/combination excited states, and then photodissociated by a second (UV) photon. The UV photons also serve to tag photoproducts by MPI.

High-resolution VMP not only supplies the high-resolution spectroscopy of the intermediate overtone states, but unravels finer details of intramolecular rotation–vibration interactions which influences the dynamics of the excited molecules (enhancement of photodissociation yield, variation of branching ratio among photoproducts, introduction of the three-body decay, *etc.*).

Halogenated hydrocarbons

Rosenwaks' group studied the ultraviolet ($\sim$235/243.135 nm) photodissociation of the fundamental symmetric and/or overtones of the CH_3 stretch of CHF_2Cl,[79] $CHFCl_2$,[80] CH_3CF_2Cl,[81] and CH_3CFCl_2.[82,83] The UV wavelengths tag the $^{35}Cl\,(^2P_j)$ and $^{37}Cl\,(^2P_j)$, or H photofragments by REMPI. In the case of CHF_2Cl,[79] molecules excited *via* stretch–bend polyad ($N = 3$, 7/2 and 4) were dissociated by UV photons.†

† The C–H stretch–bend polyad components are the complex mixture of stretching and bending modes labeled by the quantum number $N = v_s + 1/2v_a + 1/2v_b$ (v_s is the number of the pure stretching state, v_a is the quantum number for the first bending and v_b for the second).

Action spectra for Cl/Cl* fragments revealed vibrational redistribution times in the range of 1–18 ps. Chen *et al.*[80] showed the evidence for the onset of three-body decay in photodissociation of vibrationally excited $CHFCl_2$.

For CH_3CF_2Cl[81] and CH_3CFCl_2,[82,83] VMP experiments *via* 3, 4 and 5 quanta of CH stretch + ~235 nm were performed. The initial vibrational state preparation not only enhances C–Cl and C–H bond cleavage but also affects the Cl*/Cl branching ratio, as compared to the nearly isoenergetic one-photon 193 nm photolysis of the vibrationless ground state. Photofragmant yield enhancement for H, Cl and Cl* were 1.0, 1.5, 1.8, respectively, for $3\nu_{CH}$ VMP, and 3.5, 3.5 and 4.7, respectively, for $4\nu_{CH}$ VMP. The Cl*/Cl branching ratio on $3\nu_{CH}$ and $4\nu_{CH}$ VMP was, respectively, 0.54 and 0.55 (to be compared with 0.25 of direct photodissociation) for CH_3CF_2Cl,[81] and 0.49 and 0.46 (to be compared with 0.22 of direct photodissociation) for CH_3CFCl_2.[82]

Acetylene

Sheng *et al.*[84] studied VMP of acetylene in the region of $4\nu_{CH}$ (around 12 676 cm^{-1}) + 243.135 nm, probing the yield of H atoms. It was found that the (1030^00^0) IR bright state of the third C–H stretch overtone (excited with four CH stretching quanta, one symmetric and three antisymmetric) has a smaller photodissociation cross section than the (1214^00^0) combination band containing *trans*-bend mode excitation and lying in its vicinity, due to a favorable Franck–Condon factor for the latter.

Ammonia

VMP of ammonia was studied by Crim's group.[85–87] Bach *et al.*[85] used VMP action spectra to measure the rotation–vibrational spectra (2.3–3.0 μm) of ammonia in the electronic ground state. They detected the emission of electronically excited $NH_2(\tilde{A}\,^2A_1)$ produced by the photodissociation of vibrationally excited molecules. Isoenergetic photolysis of ammonia molecules with one quantum of antisymmetric N–H stretching (ν_3) or two quanta of bend ($2\nu_4$) produced three times more $NH_2(\tilde{A}\,^2A_1)$ than photolysis of molecules with a quantum of symmetric N–H stretch (ν_1) excitation. They[86] determined the vibronic structure and photodissociation dynamics of the $\tilde{A}$ state of ammonia. Initial vibrational excitation in the electronic ground state of ammonia changes the Franck–Condon factors for the subsequent electronic transitions markedly and allows assignments of sharp resonances to a progression in the degenerate bending mode. The simulation of the vibronic band envelopes provides band origins and homogeneous rovibronic bandwidths for states containing the umbrella and bending modes. The lifetimes of the bending states decreased monotonically with excess energy from 115 fs for 4^1 to 13 fs for 4^4 vibronic states in the $\tilde{A}$ state of ammonia. Rotational excitation of the recoiling NH_2 products was also reported (Fig. 3).[87]

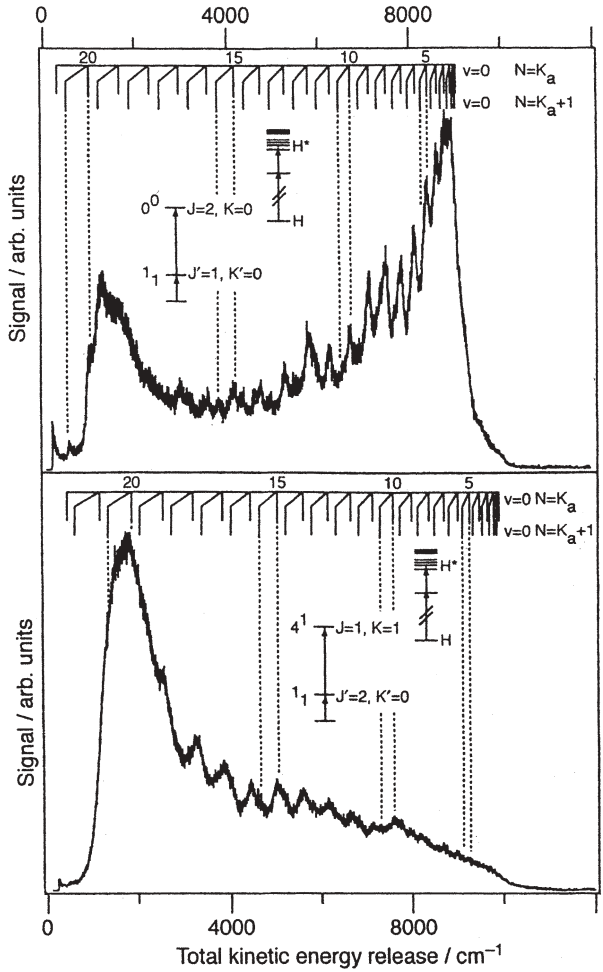

Fig. 3 Total kinetic energy release spectrum for the H + NH_2 fragments resulting from vibrationally mediated dissociation of $\tilde{A}$ state ammonia from the 0^0 ($J = 2$, $K = 0$) level at a total energy of 47 032 cm^{-1} (top) and the 4^1 ($J = 1$, $K = 1$) level at a total energy of 46 208 cm^{-1} (bottom). The combs above the spectra mark the corresponding internal energies of the $NH_2(\tilde{X})$ fragments. The spectrum (b) shows an inverted rotational population distribution with only levels $N \sim K_a > 6$ populated. (Reprinted with permission from *J. Chem. Phys.*, 2003, **118**, 7144.[87])

14 Ozone O_3

Photodissociation of ozone continues to attract a great deal of current attention in relation to the ozone depression issue. In the Hartley band, ozone primarily dissociates through the spin conserved channels,

$$O_3 + h\nu \rightarrow O_2(a\,^1\Delta_g) + O(^1D_2) \qquad (14.1)$$

$$O_3 + h\nu \rightarrow O_2(X\,^3\Sigma_g^-) + O(^3P_{2,1,0}) \quad (14.2)$$

Dylewski *et al.*[88] probed the $O(^1D_2)$ fragment in the photodissociation in the Hartley band (UV) at eight wavelengths between 235 and 305 nm, the last wavelength being close to the threshold of the reaction (14.1). The corresponding vibrational populations of $O_2(^1\Delta_g)$ were peaked at $v = 0$. The spatial anisotropy parameter β changed monotonically from about 1.2 at 235 nm to 1.7 at 298 nm. If the excited ozone molecule were to dissociate from the same geometry as the ground state (the O–O–O angle of 116.8°), the value of β close to 1.18 is to be expected. The $\boldsymbol{v}$–$\boldsymbol{J}$ correlations were reflected in the $O(^1D_2)$ $|m_j|$ populations, where m_j is the projection of the angular momentum along the relative velocity vector of the dissociating fragments. The peak at $|m_j| = 0$ indicated a parallel, incoherent excitation, expected for excitation to a single dissociative state of A′ symmetry, and substantial bending of the ozone molecule before dissociation.

Chakraborty and Bhattacharya[89] addressed the issue of enrichment of heavier isotopomer in stratospheric ozone. They studied $^{16}O/^{17}O/^{18}O$ mass-dependent photodissociation in the visible region (Chappuis band, probed at 520 and 630 nm) and in the UV (Hartley band, probed at 253.6 and 184.9 nm). In the former region, only (14.2) occurs. In the UV region, both channels (14.1) and (14.2) are operative, and moreover, the $O(^1D)$-mediated dissociation channels

$$O(^1D) + O_3 \rightarrow 2O_2 \quad (14.3)$$

$$\rightarrow 2O(^3P) + O_2 \quad (14.4)$$

complicate the situation. These authors gave the covariation plot $\Delta\delta(^{17}O)/\Delta\delta(^{18}O)$ in both regions. The slope of the plot was 0.54 ± 0.01 in the visible, expected for the mass-dependent process while the slope in the UV region was 0.63 ± 0.01, showing the contributions of both the mass-independent (pure) dissociation channels and the mass-dependent $O(^1D)$-mediated dissociation channels.

15 Other compounds

There are still many more "molecules of interest". A few research works are listed here.

Symmetric chlorine dioxide ClO_2 has been the target of a wealth of experimental and theoretical studies, because of its presumed influence on polar ozone. Delmdahl *et al.*[90] applied the velocity map imaging technique on the dissociation of ClO_2 highly photoexcited into the (24, 0, 0) vibronic level of the first excited $^2A_2$ state. The recoil of the $ClO(X\,^2\Pi)$ and $O(^3P)$ fragments was highly anisotropic. The available energy was channeled almost entirely into CO vibration. The excess energy was focused only in the three highest possible CO vibrational levels $v = 18$–20. This was attributed to a virtually linear geometry of the decaying parent evolving along the (close-lying) $^2A_1$ potential energy surface.

Photodissociation dynamics of the S_2 state of methyl nitrite (CH_3ONO) was studied by Yin *et al.*[91] The molecule was irradiated at 266 nm, and the product $NO(X\,^2\Pi, v = 0$–$3)$ was detected by LIF. The rotational distributions were quite hot.

Ethyl ethynyl ether ($HC{\equiv}COCH_2CH_3$) is an interesting molecule. Krisch *et al.*[92]

studied photodissociation at 193 nm. Only the cleavage of the C–O bond to form C_2HO radical and C_2H_5 (ethyl radical) was observed. The C_2HO radical was formed in two distinct channels, one with higher and the other with lower recoil kinetic energy. They were respectively attributed to ketenyl (HCCO) product in $\tilde{X}\,(^2A'')$ or $\tilde{A}\,(^2A')$ state, and those in a spin-forbidden $\tilde{a}\,(^4A'')$ state.

ClN_3 was photodissociated at 203 nm (Hansen *et al.*[93]). Images of state-selected $N_2(X\,^1\Sigma_g^+,\ v = 0,\ J = 68)$ was used to characterize the internal energy of the photofragments.

$$ClN_3 + h\nu \rightarrow N_2(X\,^1\Sigma_g^+) + NCl(a\,^1\Delta) \qquad (15.1)$$

$$\rightarrow N_2(X\,^1\Sigma_g^+) + NCl(X\,^3\Sigma^-). \qquad (15.2)$$

Velocity-map imaging study of the $O(^3P) + N_2$ product channel following 193 nm photolysis of N_2O was performed by Brouard *et al.*[94] About 60% of available energy appeared in product translation.

16 Vector correlations

Besides the energetic content, spatial distributions of fragments on polarized laser excitation of the parent molecules are frequently studied. The anisotropy parameter β supplies the information of the parallel/perpendicular nature of the absorption transition moment to the polarization of the exciting light. It shows the promptness of dissociation event, *i.e.* whether or not the dissociating molecule have the time to rotate before the dissociation.

Correlation between the fragment velocity vector $\boldsymbol{V}$ and rotational angular momentum vector $\boldsymbol{J}$ (the $\boldsymbol{V}$–$\boldsymbol{J}$ correlation) can provide insight to the torques on the departing fragments during dissociation. Although they have initially been applied to direct dissociation processes, even in purely statistical dissociation that is well described by the phase-space theory (PST), one can expect $\boldsymbol{V}$–$\boldsymbol{J}$ correlation as a consequence of energy and momentum conservations. McGivern and North[50] investigated this aspect on the photodissociation of NCNO, which is known as a prototypical case of statistical dissociation. Of particular interest is whether the $\boldsymbol{V}$–$\boldsymbol{J}$ correlation can provide insight into the role of the $\boldsymbol{K}$-rotor energy, *i.e.*, whether the $\boldsymbol{K}$-rotor should be treated as adiabatic, requiring its angular momentum to be conserved throughout the reaction, or whether it should be allowed to couple into the reaction coordinate. Doppler spectroscopy experiments were performed to measure state-selected CN scalar and vector correlations at 520 and 532 nm. These authors found that the correlated vibrational and rotational distributions could be well described using separate statistical ensembles/phase space theory (SSE/PST), if the $\boldsymbol{K}$-rotor was considered inactive. This is indicative of approximate $\boldsymbol{K}$-scrambling at the transition state.

Hydrogen peroxide is noted for the "cartwheel" rotation of the two OH fragments, keeping with the angular momentum conservation law. Alexander[95] photodissociated hydrogen peroxide at 355 nm, the wavelength far from its absorption maximum, using both linearly and circularly polarized light. This wavelength corresponds to the long wavelength tail of the ultraviolet absorption band. The effects of dynamical

torsion and parent molecule bending vibrations on product rotational alignment were discussed, and gave the evidence supporting preferential dissociation of ground-state molecules far from the equilibrium configuration.

17 van der Waals molecules and clusters

The intriguing nature of $(NO)_2$ is that it belongs to the special family of weakly bound complexes that are covalently bound in the ground state ($D_0 = 710 \pm 15\ cm^{-1}$). UV photodissociation of $(NO)_2$ was studied in detail by Reisler and coworkers.[96]

$$(NO)_2 + h\nu \rightarrow NO\,(A\,^2\Sigma^+) + NO\,(X\,^2\Pi) \qquad (17.1)$$

They measured angular distributions of selected rotational states of NO ($A\,^2\Sigma^+$, $v = 0$) products obtained in the 213 nm photodissociation of $(NO)_2$. The recoil anisotropy parameter of the photofragments (β_{eff}) decreased significantly at low center-of-mass translational energy (E_T) from its maximum value of 1.36 ± 0.05. They explained such a variation by considering a classical model that takes into account the transverse recoil component mandated by angular momentum conservation. For most of the center-of-mass translational energy range, both co-rotating and counter-rotating fragments are produced, but at the lowest energies, only the latter is allowed. Suzuki's group[97] studied the UV photodissociation of $(NO)_2$ using femtosecond charged particle imaging. Inokuchi *et al.*[98] reported on IR photodissociation spectroscopy of $[aniline–(water)_n]^+$ ($n = 1$–8). The $n = 1$ ion was shown to have an N–H···O hydrogen bond. For the $n = 3$ ion, the calculated spectrum of the 2–1 branched structure coincided well with the observed one. The $n = 6$–8 ions showed features quite different from those of the $n = 1$–5 ions. Proton-transferred structures were suggested for $n = 6$–8 ions.

18 Metal complexes

Photodissociation of metal (monovalent positive ion M^+)-containing molecules attract much attention. Usually, photodissociation products are detected by mass spectrometer, mostly of the time-of flight type. Elimination of one or more ligand(s) was found to be the dominant channel. Fragmentation of ligand(s) is observed in some cases. In many cases the major products are metal ions.

Action spectra of fragment(s) provide the absorption spectra of the complexes. This method is denoted photodissociation spectroscopy and leads to the elucidation of the nature of metal–ligand bonds. Some are covalent, and some are very weak, corresponding to solvated complexes in solution. The elimination of ligand(s) is sometimes called "evaporation", in the latter case.

Magnesium complexes have received the attention of many research groups. In the photodissociation of Mg^+–formaldehyde, Kleiber and coworkers[99] obtained MgH^+ along with Mg^+. Yang and coworkers[100] studied diethylamine and triethylamine complexes. In the latter case, charge-transfer (CT) products $N^+(C_2H_5)_3$ and $(C_2H_5)_2N^+CH_2$ were obtained, together with Mg^+ and $Mg^+N(C_2H_5)CH_3$. Acrylonitrile clusters, $Mg^+(CH_2{=}CHCN)_n$ ($n = 1$–10), were studied by Furuya *et al.*[101] They obtained photodissociation spectra for $n = 1$, 2, and photofragment

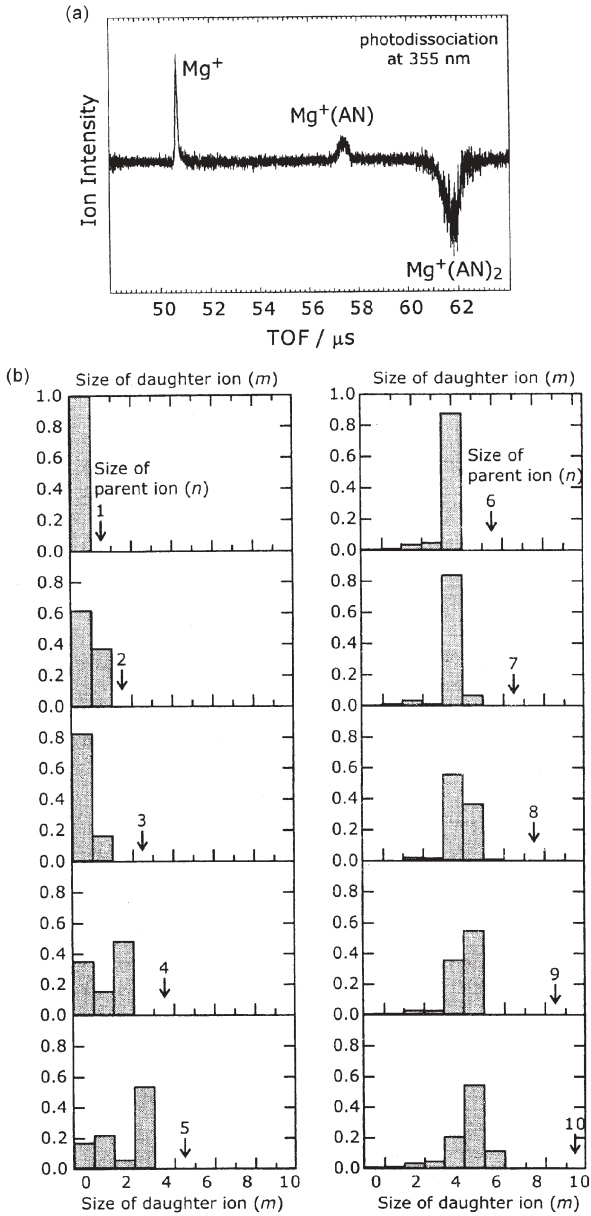

Fig. 4 The photodissociation difference mass spectra from the photolysis laser on-minus-off of $Mg^+(AN)_2$ (a), and branching ratios of fragment ions produced by photolysis of $Mg^+(AN)_n$ (n = 1–10) at the dissociation wavelength of 355 nm. AN stands for acrylonitrile. (Reprinted with permission from *J. Chem. Phys.*, 2003, **118**, 5456.[101])

Table 1 Photodissociation of metal complexes

Metal:ligand	Wavelength/ wavenumber	Method	Detected species	Ref.
Mg^+H_2CO	16 660–45 450 cm^{-1}	PDS[a]	Mg^+, MgH^+	99
$Mg^+NH(C_2H_5)_2$	230–440 nm	PDS	Mg^+, Mg^+NHCH_3, $(C_2H_5)HN^+CHCH_3$	100
$Mg^+N(C_2H_5)_3$	230–440 nm	PDS	Mg^+, $Mg^+N(C_2H_5)CH_3$, $N^+(C_2H_5)_3$, $(C_2H_5)_2N^+CH_2$	100
$Mg^+(CH_2{=}CHCN)_n$ (n = 1, 2)	20 000–45 000 cm^{-1}	PDS	Evap.[b]	101
$Mg^+(CH_2{=}CHCN)_n$ (n = 1–10)	355 nm		Evap.	101
$Mg^+OCNC_2H_5$	230–410 nm	PDS	Mg^+, Mg^+OCN	102
$Mg^+(NCCH_3)_n$ (n = 1–4)	240–540 nm	PDS	Evap., Mg^+, Mg^+NC	103
$Mg^+(CO_2)_n$ (n = 2–6)	2300–2450 cm^{-1}	IRPDS	Evap.	104
$Mg^+(CO_2)_nAr$ (n = 1–3)	2300–2450 cm^{-1}	IRPDS	$Mg^+(CO_2)_n$	104
Mg^+NH_3	26 000–41 000 cm^{-1}	PDS	Mg^+, Mg^+NH_2, NH_3^+ (charge transfer product)	105
$Mg^+(NH_3)_n$ (n = 2)	26 000–41 000 cm^{-1}	PDS	Mg^+, Mg^+NH_2, $Mg^+NH_2NH_3$, Mg^+NH_3	106
$Mg^+(NH_3)_n$ (n = 3, 4)	26 000–41 000 cm^{-1}	PDS	Evap.	106
$Al^+C_2H_4$	32 000–46 000 cm^{-1}	PDS	Al^+, $C_2H_4^+$	107
$Al^+C_3H_6$	32 000–46 000 cm^{-1}	PDS	Al^+, $C_3H_6^+$	107
$Al^+(1\text{-}C_4H_8)$	32 000–46 000 cm^{-1}	PDS	Al^+, $(1\text{-}C_4H_8)^+$	107
Al^+CH_3CHO	29 000–46 000 cm^{-1}	PDS	Al^+	108
$Al^+C_6H_6$	600–1800 cm^{-1}	IRPDS	Al^+	109
Ca^+Ar_2	13 890–14 240 cm^{-1}	PDS	Ca^+Ar	110
Ca^+HCHO	14 000–36 000 cm^{-1}	PDS	Ca^+	111
$Fe^+(CO_2)_n$	2050–4500 cm^{-1}	IRPDS	Loss of one CO_2	112
$Fe^+(CO_2)_nAr$	2050–4500 cm^{-1}	IRPDS	Loss of Ar	112
$Fe^+(CO_2)_n$ (n = 2–14)	2000–4500 cm^{-1}	IRPDS	Successive elimination of CO_2	113
$Fe^+(CO_2)_nAr_m$	2000–4500 cm^{-1}	IRPDS		113
Zn^+CH_4	227–263 nm	PDS	Zn^+CH_3 (major), CH_3^+, Zn^+, ZnH^+	114
$Zn^+C_2H_4$	220–550 nm	PDS	Zn^+, $C_2H_4^+$ (major), $C_2H_3^+$, $C_2H_2^+$ (<250 nm)	115
Sr^+CO	19 000–23 000 cm^{-1}	PDS	Sr^+	116
Sr^+CO	15 600–16 200 cm^{-1}	PDS		117
$Sr^+(CH_3OH)_n$, $Sr^+(CH_3OD)_n$ (n = 1–4)	310–1500 nm	PDS		118
$Sr^+(CH_3OD)$,	561 nm		Sr^+ (−L),[c] $SrOD^+$ (−Me), $SrOCH_3^+$ (−D)	118
$Sr^+(CH_3OD)_2$,	588 nm		−L, −Me, −D, −2L, −(L + Me), −(L + D)	118
$Sr^+(CH_3OD)_3$	594 nm		−L, −D, −2L, −(L + Me), −(L + D), −(2L + Me), −(2L + D)	118
$Sr^+(CH_3OD)_3$	780 nm		−L, −D, −2L, −(L + Me), −(L + D)	118
$Sr^+(CH_3OD)_4$	656 nm		−L, −2L, −(L + Me), −(L + D), −(2L + Me), −(2L + D), −3L	118

Table 1 Photodissociation of metal complexes (*Continued*)

Metal:ligand	Wavelength/ wavenumber	Method	Detected species	Ref.
Cu^+(furan)	355 nm	PDS	$Furan^+$	119
Ag^+(furan)	355 nm	PDS	$Furan^+$	119
Au^+(furan)	355 nm	PDS	$Furan^+$, $C_3H_4^+$	119

[a] Photodissociation spectroscopy. [b] Evaporation of ligand(s). [c] −L = loss of one ligand (CH_3OD), −D = loss of one D atom, −Me = loss of one methyl group (CH_3).

mass spectra (at 355 nm) for $n = 1$–10 (Fig. 4). Sun *et al.*[102] studied the Mg^+–ethyl isocyanate complex $Mg^+OCNC_2H_5$. Apart from the persistent product Mg^+, Mg^+OCN and $C_2H_5^+$ were obtained as photoproducts.

Acetonitrile clusters $(Mg^+(NCCH_3)_n$ ($n = 1$–4), were investigated by Yang's group[103] in the 230–560 nm range. The photodissociation products were mostly Mg^+ and nonreactive evaporation fragments. Duncan and coworkers[104] used an IR optical parametric oscillator/optical parametric amplifier (OPO/OPA) laser for IR photodissociation spectroscopy of $Mg^+(CO_2)_n$ and $Mg^+(CO_2)_n$ Ar clusters. Complexes of Mg^+ with ammonia and ammonia clusters $Mg^+(NH_3)_n$ were studied at 355 nm by Fuke and coworkers.[105,106] For $n = 1$, they obtained Mg^+, Mg^+NH_2 and NH_3^+ (a CT product). For $n > 3$, however, only evaporation products were observed.

Kleiber's group studied Al^+ complexes with ethene, propene and butane,[107] and with acetaldehyde.[108] Meijer, Duncan and coworkers used a tunable free electron laser (FEL) to obtain the IR spectrum of $Al^+C_6H_6$.[109]

Duncan and coworkers[110] studied Ca^+Ar_2 complexes. Photodissociation spectra were analyzed to infer the structure of the complex (linear or bent). It was found that the complex is most likely linear. Lu *et al.* of Kleiber's group[111] investigated the photodissociation spectroscopy of Ca^+–formaldehyde. A C_{2v} ground-state geometry with a bond dissociation energy D_e'' (Ca^+–OCH_2) = 0.9 ± 0.2 eV was obtained.

IR photodissociation of $Fe^+(CO_2)_n$ and $Fe^+(CO_2)_nAr$ was investigated by Duncan's group[112,113] in the wavenumber range 2050–4500 cm^{-1}. Successive loss of CO_2 ligands was observed for $Fe^+(CO_2)_n$, and loss of Ar for $Fe^+(CO_2)_nAr_m$. In a series of $Fe^+(CO_2)_n$ complexes ($n = 2$–14), the asymmetric CO stretch band showed a blue shift compared to the free CO_2. The blue shift decreased initially with cluster size, but became nearly constant after $n = 4$. The photochemistry of Zn, Sr, Cu, Ag and Au complexes were also investigated.[114–119] Photodissociation studies of metal complexes are listed in Table 1.

References

1 H. Sato, *Chem. Rev.*, 2001, **101**, 2687.
2 H. Okabe, *Photochemistry of Small Molecules*, Wiley, New York, 1978.
3 *Molecular Photodissociation Dynamics*, ed. M. N. R. Ashfold and J. E. Baggott, Royal Society of Chemistry, London, 1987.
4 R. Schinke, *Photodissociation Dynamics*, Cambridge University Press, Cambridge, 1993.
5 M.-F. Lin, C.-L. Huang, V. V. Kislov, A. M. Mebel, Y. T. Lee and C.-K. Ni, *J. Chem. Phys.*, 2003, **119**, 7701.
6 S. M. Wu, J. J. Lin, Y. T. Lee and X. Yang, *J. Chem. Phys.*, 2000, **112**, 8027.
7 C. C. Wang, Y. T. Lee, J. J. Lin, J. Shu, Y.-Y. Lee and X. Yang, *J. Chem. Phys.*, 2002, **117**, 153, and references therein.

8 J. J. Lin, C. C. Wang, Y. T. Lee and X. Yang, *J. Chem. Phys.*, 2000, **113**, 9668.
9 J. O'Reilly, S. Douin, S. Boye, N. Shafizadeh and D. Gauyacq, *J. Chem. Phys.*, 2003, **119**, 820.
10 S.-H. Lee, Y.-Y. Lee, Y. T. Lee and X. Yang, *J. Chem. Phys.*, 2003, **119**, 827.
11 M. Kono, K. Hoshina and K. Yamanouchi, *J. Chem. Phys.*, 2002, **117**, 1040.
12 N. Yamakita, S. Iwamoto and S. Tsuchiya, *J. Phys. Chem. A*, 2003, **107**, 2597.
13 S. Zamith, V. Blanchet, B. Girard, J. Andersson, S. L. Sorensen, I. Hjelte, O. Björneholm, D. Gauyacq, J. Norin, J. Mauritsson and A. L'Huillier, *J. Chem. Phys.*, 2003, **119**, 3763.
14 R. H. Qadiri, E. J. Feltham, E. E. H. Cottrill, N. Taniguchi and M. N. R. Ashfold, *J. Chem. Phys.*, 2002, **116**, 906.
15 S. Harich, J. J. Lin, Y. T. Lee and X. Yang, *J. Chem. Phys.*, 2000, **112**, 6656.
16 R. H. Qadiri, E. J. Feltham, N. H. Nahler, R. P. Garcia and M. N. R. Ashfold, *J. Chem. Phys.*, 2003, **119**, 12842.
17 J. J. Lin, Y. Chen, Y. Y. Lee, Y. T. Lee and X. Yang, *Chem. Phys. Lett.*, 2002, **361**, 374.
18 A. Läuter, D. Suresh and H.-R. Volpp, *J. Chem. Phys.*, 2003, **118**, 5821.
19 J. Huang, D. Xu, W. H. Fink and W. M. Jackson, *J. Chem. Phys.*, 2001, **115**, 6012.
20 D. Xu, J. S. Francisco, J. Huang and W. M. Jackson, *J. Chem. Phys.*, 2002, **117**, 2578.
21 J. Huang, D. Xu, J. S. Francisco and W. M. Jackson, *J. Chem. Phys.*, 2003, **118**, 3083.
22 P. Zou, W. S. McGivern, O. Sorkhabi, A. G. Suits and S. W. North, *J. Chem. Phys.*, 2000, **113**, 7149.
23 Y.-R. Lee, C.-C. Chen and S.-M. Lin, *J. Chem. Phys.*, 2003, **118**, 10494.
24 P. Farmanara, V. Stert, H.-H. Ritze and W. Radloff, *J. Chem. Phys.*, 2000, **113**, 1705.
25 W. G. Roeterdink and M. H. M. Janssen, *J. Chem. Phys.*, 2002, **117**, 6500.
26 S. T. Park, S. K. Kim and M. S. Kim, *Nature*, 2002, **415**, 306.
27 S. T. Park and M. S. Kim, *J. Chem. Phys.*, 2002, **117**, 124.
28 S.-R. Lin, S.-C. Lin, Y.-C. Lee, Y.-C. Chou, I.-C. Chen and Y.-P. Lee, *J. Chem. Phys.*, 2001, **114**, 160.
29 D.-K. Liu, L. T. Letendre and H.-L. Dai, *J. Chem. Phys.*, 2001, **115**, 1734.
30 C.-Y. Wu, C.-Y. Chung, Y.-C. Lee and Y.-P. Lee, *J. Chem. Phys.*, 2002, **117**, 9785.
31 D. E. Szpunar, Y. Liu, M. J. McCullagh, L. J. Butler and J. Shu, *J. Chem. Phys.*, 2003, **119**, 5078.
32 S.-T. Tsai, C.-K. Lin, Y. T. Lee and C.-K. Ni, *J. Chem. Phys.*, 2000, **113**, 67.
33 S.-T. Tsai, C.-K. Lin, Y. T. Lee and C.-K. Ni, *Rev. Sci. Instrum.*, 2001, **72**, 1963.
34 S.-T. Tsai, Y. T. Lee and C.-K. Ni, *J. Phys. Chem. A*, 2000, **104**, 10125.
35 S.-T. Tsai, C.-L. Huang, Y. T. Lee and C.-K. Ni, *J. Chem. Phys.*, 2001, **115**, 2449.
36 C.-L. Huang, J.-C. Jiang, A. M. Mebel, Y. T. Lee and C.-K. Ni, *J. Am. Chem. Soc.*, 2003, **125**, 9814.
37 C.-L. Huang, J.-C. Jiang, S. H. Lin, Y. T. Lee and C.-K. Ni, *J. Chem. Phys.*, 2002, **116**, 7779.
38 C.-L. Huang, J.-C. Jiang, Y. T. Lee and C.-K. Ni, *J. Chem. Phys.*, 2002, **117**, 7034.
39 M. Kadi and J. Davidsson, *Chem. Phys. Lett.*, 2003, **378**, 172.
40 C.-K. Lin, C.-L. Huang, J.-C. Jiang, A. H. H. Chang, Y. T. Lee, S. H. Lin and C.-K. Ni, *J. Am. Chem. Soc.*, 2002, **124**, 4068.
41 M.-F. Lin, C.-L. Huang, Y. T. Lee and C.-K. Ni, *J. Chem. Phys.*, 2003, **119**, 2032.
42 Y.-R. Lee, C.-C. Chen and S.-M. Lin, *J. Chem. Phys.*, 2003, **118**, 9073.
43 Y.-M. Li, J.-L. Sun, H.-M. Yin, K.-L. Han and G.-Z. He, *J. Chem. Phys.*, 2003, **118**, 6244.
44 R. Seiler and B. Dick, *Chem. Phys.*, 2003, **288**, 43.
45 M. D. Poulsen, E. Skovsen and H. Stapelfeldt, *J. Chem. Phys.*, 2002, **117**, 2097.
46 P. A. Cook, S. R. Langford, M. N. R. Ashfold and R. N. Dixon, *J. Chem. Phys.*, 2000, **113**, 994.
47 C. Y. Oh, S. K. Shin, H. L. Kim and C. R. Park, *Chem. Phys. Lett.*, 2002, **363**, 404.
48 C. Y. Oh, S. K. Shin, H. L. Kim and C. R. Park, *J. Phys. Chem. A*, 2003, **107**, 4333.
49 Q. Li, R. T. Carter and J. R. Huber, *Chem. Phys. Lett.*, 2000, **323**, 105.
50 W. S. McGivern and S. W. North, *J. Chem. Phys.*, 2002, **116**, 7027.
51 P. Li, L. K. Wong and W. Y. Fan, *Chem. Phys. Lett.*, 2003, **380**, 117.
52 E. J. Feltham, R. H. Qadiri, E. E. H. Cottrill, P. A. Cook, J. P. Cole, G. G. Balint-Kurti and M. N. R. Ashfold, *J. Chem. Phys.*, 2003, **119**, 6017.
53 Y. Chen and L. Zhu, *J. Phys. Chem. A*, 2003, **107**, 4643.
54 M.-W. Chen, S. J. Lee and I.-C. Chen, *J. Chem. Phys.*, 2003, **119**, 8347.
55 E. W.-G.. Diau, C. Kötting and A. H. Zewail, *Chem. Phys. Chem.*, 2001, **2**, 273.
56 E. W.-G.. Diau, C. Kötting and A. H. Zewail, *Chem. Phys. Chem.*, 2001, **2**, 294.
57 E. W.-G.. Diau, C. Kötting, T. I. Sølling and A. H. Zewail, *Chem. Phys. Chem.*, 2002, **3**, 57.
58 T. I. Sølling, E. W.-G.. Diau, C. Kötting, S. DeFeyter and A. H. Zewail, *Chem. Phys. Chem.*, 2002, **3**, 79.
59 W.-K. Chen, J.-W. Ho and P.-Y. Cheng, *Chem. Phys. Lett.*, 2003, **380**, 411.
60 X.-P. Tang, S.-F. Wang, M. E. Elshakre, L.-R. Gao, Y.-L. Wang, H.-F. Wang and F.-A. Kong, *J. Phys. Chem. A*, 2003, **107**, 13.
61 S. M. Clegg, B. F. Parsons, S. J. Klippenstein and D. L. Osborn, *J. Chem. Phys.*, 2003, **119**, 7222.
62 Q. Zhong, D. A. Steinhurst, A. P. Baronavski and J. C. Owrutsky, *Chem. Phys. Lett.*, 2003, **370**, 609.
63 H. P. Upadhyaya, A. Kumar and P. D. Naik, *J. Chem. Phys.*, 2003, **118**, 2590.
64 S. Dhanya, D. K. Maity, H. P. Upadhyaya, A. Kumar, P. D. Naik and R. D. Saini, *J. Chem. Phys.*, 2003, **118**, 10093.
65 V. Dribinski, A. B. Potter, A. V. Demyanenko and H. Reisler, *J. Chem. Phys.*, 2001, **115**, 7474.

66 A. B. Potter, V. Dribinski, A. V. Demyanenko and H. Reisler, *Chem. Phys. Lett.*, 2001, **349**, 257.
67 L. Feng, X. Huang and H. Reisler, *J. Chem. Phys.*, 2002, **117**, 4820.
68 L. Feng, A. V. Demyanenko and H. Reisler, *J. Chem. Phys.*, 2003, **118**, 9623.
69 A. A. Hoops, R. T. Bise, J. R. Gascooke and D. M. Neumark, *J. Chem. Phys.*, 2001, **114**, 9020.
70 S. Gómez, H. M. Lambert and P. L. Houston, *J. Phys. Chem. A*, 2001, **105**, 6342.
71 R. C. Richter, V. I. Khamaganov and A. J. Hynes, *Chem. Phys. Lett.*, 2000, **319**, 341.
72 F. Sun, J. P. Glass and R. F. Curl, *Chem. Phys. Lett.*, 2001, **337**, 72.
73 H.-S. Im and E. B. Bernstein, *J. Phys. Chem. A*, 2002, **106**, 7565.
74 D. Stolyarov, E. Polyakova, I. Bezel and C. Wittig, *Chem. Phys. Lett.*, 2002, **358**, 71.
75 B. Abel, S. Y. Grebenshchikov, R. Schinke and D. Schwarzer, *Chem. Phys. Lett.*, 2003, **368**, 252.
76 C. Morrell, C. Breheny, V. Haverd, A. Cawley and G. Hancock, *J. Chem. Phys.*, 2002, **117**, 11121.
77 P. Zou, J. Park, B. A. Schmitz, T. Nguyen and S. W. North, *J. Phys. Chem. A*, 2002, **106**, 1004.
78 R. Soller, J. M. Nicovich and P. H. Wine, *J. Phys. Chem. A*, 2002, **106**, 8378, and references therein.
79 L. Li, G. Dorfman, A. Melchior, S. Rosenwaks and I. Bar, *J. Chem. Phys.*, 2002, **116**, 1869.
80 X. Chen, R. Marom, S. Rosenwaks, I. Bar, T. Einfeld, C. Maul and K.-H. Gericke, *J. Chem. Phys.*, 2001, **114**, 9033.
81 G. Dorfman, A. Melchoir, S. Rosenwaks and I. Bar, *J. Phys. Chem. A*, 2002, **106**, 8285.
82 A. Melchior, X. Chen, I. Bar and S. Rosenwaks, *J. Chem. Phys.*, 2000, **112**, 10787.
83 T. Einfeld, C. Maul, K.-H. Gericke, R. Marom, S. Rosenwaks and I. Bar, *J. Chem. Phys.*, 2001, **115**, 6418.
84 X. Sheng, Y. Ganot, S. Rosenwaks and I. Bar, *J. Chem. Phys.*, 2002, **117**, 6511.
85 A. Bach, J. M. Hutchison, R. J. Holiday and F. F. Crim, *J. Chem. Phys.*, 2002, **116**, 4955.
86 A. Bach, J. M. Hutchison, R. J. Holiday and F. F. Crim, *J. Chem. Phys.*, 2002, **116**, 9315.
87 A. Bach, J. M. Hutchison, R. J. Holiday and F. F. Crim, *J. Chem. Phys.*, 2003, **118**, 7144.
88 S. M. Dylewski, J. D. Geiser and P. L. Houston, *J. Chem. Phys.*, 2001, **115**, 7460.
89 S. Chakraborty and S. K. Bhattacharya, *J. Chem. Phys.*, 2003, **118**, 2164.
90 R. F. Delmdahl, B. L. G. Bakker and D. H. Parker, *J. Chem. Phys.*, 2000, **112**, 5298.
91 H.-M. Yin, J.-L. Sun, Y.-M. Li, K.-L. Han, G.-Z. He and S.-L. Cong, *J. Chem. Phys.*, 2003, **118**, 8248.
92 M. J. Krisch, J. L. Miller, L. J. Butler, H. Su, R. Bersohn and J. Shu, *J. Chem. Phys.*, 2003, **119**, 176.
93 N. Hansen, A. M. Wodtke, A. V. Komissarov and M. C. Heaven, *Chem. Phys. Lett.*, 2003, **368**, 568.
94 M. Brouard, A. P. Clark, C. Vallance and O. S. Vasyutinskii, *J. Chem. Phys.*, 2003, **119**, 771.
95 A. Alexander, *J. Chem. Phys.*, 2003, **118**, 6234.
96 A. V. Demyanenko, A. B. Potter, V. Dribinski and H. Reisler, *J. Chem. Phys.*, 2002, **117**, 2568.
97 M. Tsubouchi, C. A. deLange and T. Suzuki, *J. Chem. Phys.*, 2003, **119**, 11728.
98 Y. Inokuchi, K. Ohashi, Y. Honkawa, N. Yamamoto, H. Sekiya and N. Nishi, *J. Phys. Chem. A*, 2003, **107**, 4230.
99 W.-Y. Lu, T.-H. Wong, Y. Sheng and P. D. Kleiber, *J. Chem. Phys.*, 2002, **117**, 6970 (*J. Chem. Phys,* 2003, **118**, 5267) (erratum).
100 W. Guo, H. Liu and S. Yang, *J. Chem. Phys.*, 2002, **116**, 2896.
101 A. Furuya, K. Ohshimo, H. Tsunoyama, F. Misaizu, K. Ohno and H. Watanabe, *J. Chem. Phys.*, 2003, **118**, 5456.
102 J.-L. Sun, H. Liu, K.-L. Han and S. Yang, *J. Chem. Phys.*, 2003, **118**, 10455.
103 H. Liu, W. Guo and S. Yang, *J. Chem. Phys.*, 2001, **115**, 4612.
104 G. Gregoire, N. R. Brinkmann, D. van Heijnsbergen, H. F. Schaefer and M. A. Duacan, *J. Phys. Chem. A*, 2003, **107**, 218.
105 S. Yoshida, N. Okai and K. Fuke, *Chem. Phys. Lett.*, 2001, **347**, 93.
106 S. Yoshida, K. Daigoku, N. Okai, A. Takahata, A. Sabu, K. Hashimoto and K. Fuke, *J. Chem. Phys.*, 2002, **117**, 8657.
107 W.-Y. Lu, R.-G. Liu, T.-H. Wong, J. Chen and P. D. Kleiber, *J. Phys. Chem. A*, 2002, **106**, 725.
108 W.-Y. Lu, M. Acar and P. D. Kleiber, *J. Chem. Phys.*, 2002, **116**, 4847.
109 D. van Heijnsbergen, T. D. Jaeger, G. von Helden, G. Meijer and M. A. Duncan, *Chem. Phys. Lett.*, 2002, **364**, 345.
110 J. Velasquez, K. N. Kirschner, J. E. Reddic and M. A. Duncan, *Chem. Phys. Lett.*, 2001, **343**, 613.
111 W.-Y. Lu, T.-H. Wong, Y. Sheng and P. D. Kleiber, *J. Chem. Phys.*, 2003, **118**, 6905.
112 G. Gregoire, J. Verasquez and M. A. Duncan, *Chem. Phys. Lett.*, 2001, **349**, 451.
113 M. Gregoire and M. A. Duncan, *J. Chem. Phys.*, 2002, **117**, 2120.
114 W.-Y. Lu, T.-H. Wong and P. D. Kleiber, *Chem. Phys. Lett.*, 2001, **347**, 183.
115 W.-Y. Lu, P. D. Kleiber, M. A. Young and K.-H. Yang, *J. Chem. Phys.*, 2001, **115**, 5823.
116 S. C. Farantos, E. Filippou, S. Stamatiadis, G. E. Froudakis, M. Mühlhäuser, M. Massaouti, A. Sfounis and M. Velegrakis, *Chem. Phys. Lett.*, 2002, **366**, 231.
117 S. C. Farantos, E. Filippou, S. Stamatiadis, E. Froudakis, M. Mühlhäuser, M. Peric, M. Massaouti, A. Sfounis and M. Velegrakis, *Chem. Phys. Lett.*, 2003, **379**, 242.
118 J. I. Lee, J. Qian, D. C. Sperry, A. J. Midey, Jr., S. G. Donnelly and J. M. Farrer, *J. Phys. Chem. A*, 2002, **106**, 9993.
119 P.-H. Su, F.-W. Lin and C.-S. Yeh, *J. Phys. Chem. A*, 2001, **105**, 9643.